

Published as “C Lihl, B. Heckel, A. Grzybkowska, A. Dybala-Defratyka, V. Ponsin, C. Torrentó, D. Hunkeler, M. Elsner, Compound-Specific Chlorine Isotope Fractionation in Biodegradation of Atrazine, Environmental Science: Processes & Impacts 22 (2020), pp. 792 – 801; DOI: 10.1039/C9EM00503J”

## Compound-Specific Chlorine Isotope Fractionation in Biodegradation of Atrazine<sup>†</sup>

Christina Lihl<sup>a,b</sup>, Benjamin Heckel<sup>a,b</sup>, Anna Grzybkowska<sup>c</sup>, Agnieszka Dybala-Defratyka<sup>c</sup>, Violaine Ponsin<sup>d,e</sup>, Clara Torrentó<sup>d,f</sup>, Daniel Hunkeler<sup>d</sup>, Martin Elsner<sup>a,b,\*</sup>

<sup>a</sup> Institute of Groundwater Ecology, Helmholtz Zentrum München, Ingolstädter Landstraße 1, 85764 Neuherberg, Germany

<sup>b</sup> Chair of Analytical Chemistry and Water Chemistry, Technical University of Munich, Marchioninstraße 17, 81377 Munich, Germany

<sup>c</sup> Institute of Applied Radiation Chemistry, Faculty of Chemistry, Lodz University of Technology, Zeromskiego 116, 90-924 Lodz, Poland

<sup>d</sup> Centre of Hydrogeology and Geothermics (CHYN), University of Neuchâtel, 2000 Neuchâtel, Switzerland

<sup>e</sup> Département des sciences de la Terre et de l’atmosphère, Université du Québec à Montréal, 201 avenue du Président Kennedy, Montréal, QC, Canada

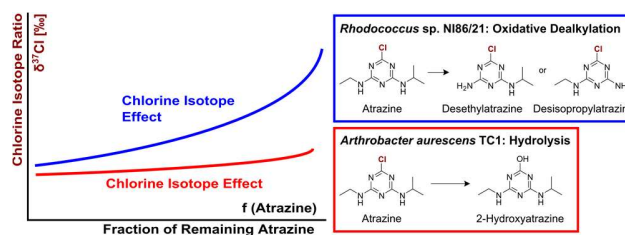
<sup>f</sup> Grup MAiMA, Departament de Mineralogia, Petrologia i Geologia Aplicada, Facultat de Ciències de la Terra, Universitat de Barcelona (UB), C/ Martí i Franquès s/n, 08028, Barcelona, Spain.

\* Corresponding Author: Phone: +49 89/2180-78231. E-mail: [m.elsner@tum.de](mailto:m.elsner@tum.de)

<sup>†</sup> Electronic Supplementary Information (ESI) available: Information concerning the HPLC temperature programs, two Figures and one Table illustrating the GC-qMS method optimization for chlorine analysis, one Table illustrating the method comparison of the GC-qMS for chlorine analysis, one Figure and one Table considering H-abstraction during chlorine CSIA, two Figures illustrating the results of HPLC concentration analysis.

KEYWORDS: hydrolysis, oxidative dealkylation, compound-specific isotope analysis, chlorine isotope effect, *Arthrobacter*, *Rhodococcus*

Graphical Abstract:



## Environmental Significance:

Atrazine is an important chlorinated micropollutant. Although degradable *via* different pathways (dealkylation and hydrolytic dechlorination), it is often recalcitrant and persists in groundwater. To assess and understand its degradation pathways, compound-specific carbon and nitrogen isotope analysis has been advanced, but information from chlorine isotope fractionation has been missing until today. This study explores the added benefit of chlorine isotope fractionation as indicator of natural atrazine transformation. Together with carbon and nitrogen isotope analysis, this enables a multi-element approach which can improve source identification and differentiation of microbial transformation pathways in the environment.

## ABSTRACT

Atrazine is a frequently detected groundwater contaminant. It can be microbially degraded by oxidative dealkylation or by hydrolytic dechlorination. Compound-specific isotope analysis is a powerful tool to assess its transformation. In previous work, carbon and nitrogen isotope effects were found to reflect these different transformation pathways. However, chlorine isotope fractionation could be a particularly sensitive indicator of natural transformation since chlorine isotope effects are fully represented in the molecular average while carbon and nitrogen isotope effects are diluted by non-reacting atoms. Therefore, this study explored chlorine isotope effects during atrazine hydrolysis with *Arthrobacter aureescens* TC1 and oxidative dealkylation with *Rhodococcus* sp. NI86/21. Dual element isotope slopes of chlorine vs. carbon isotope fractionation ( $\Lambda^{Arthro}_{Cl/C} = 1.7 \pm 0.9$  vs.  $\Lambda^{Rhodo}_{Cl/C} = 0.6 \pm 0.1$ ) and chlorine vs. nitrogen isotope fractionation ( $\Lambda^{Arthro}_{Cl/N} = -1.2 \pm 0.7$  vs.  $\Lambda^{Rhodo}_{Cl/N} = 0.4 \pm 0.2$ ) provided reliable indicators of different pathways. Observed chlorine isotope effects in oxidative dealkylation ( $\epsilon_{Cl} = -4.3 \pm 1.8$  ‰) were surprisingly large, whereas in hydrolysis ( $\epsilon_{Cl} = -1.4 \pm 0.6$  ‰) they were small, indicating that C-Cl bond cleavage was not the rate-determining step. This demonstrates the importance of constraining expected isotope effects of new elements before using the approach in the field. Overall, the triple element isotope information brought forward here enables a more reliable identification of atrazine sources and degradation pathways.

## INTRODUCTION

The herbicide atrazine has been used in agriculture to inhibit growth of broadleaf and grassy weeds<sup>1</sup>. In the U.S. atrazine was the second most commonly used herbicide in 2012 and is still in use today<sup>2</sup>. In the European Union atrazine was banned in 2004<sup>3</sup>, but together with its metabolites it is still frequently detected at high concentrations in groundwater<sup>4, 5</sup>. The massive and widespread use has led to a wide-ranging presence of atrazine in the environment, which can have harmful effects on living organisms and humans<sup>6</sup>. Therefore, the environmental fate of atrazine is of significant concern and much attention has been directed at detecting and enhancing its natural biodegradation. However, assessing microbial degradation of atrazine in the environment is challenging with conventional methods like concentration analysis. Sorption and remobilization of the parent compound and its metabolites, as well as further transformation of the metabolites inevitably lead to fluctuations in concentrations<sup>7-10</sup>, which make it difficult to assess the net extent of atrazine degradation in the field.

In recent years, compound-specific isotope analysis (CSIA) has been proposed as an alternative approach to detect and quantify the degradation of atrazine<sup>11-13</sup>.

In contrast to, and complementary to traditional methods, CSIA informs about transformation without the need to detect metabolites. The reason is that during (bio)chemical transformations molecules with heavy isotopes are typically enriched in the remaining substrate since their bonds are more stable and, therefore, usually react slower than molecules containing light isotopes (normal kinetic isotope effect). The ratios of heavy to light isotopes (e.g.  $^{13}\text{C}/^{12}\text{C}$  for carbon) in the remaining substrate, therefore, change during transformation. Observing such changes can be used as direct (and concentration-independent) indicator of degradation<sup>14, 15</sup>.

Isotope values are reported in the  $\delta$ -notation relative to an international reference material, e.g. for carbon<sup>14, 15</sup>:

$$\delta^{13}\text{C} = \left[ \left( \frac{^{13}\text{C}}{^{12}\text{C}} \right)_{\text{Sample}} - \left( \frac{^{13}\text{C}}{^{12}\text{C}} \right)_{\text{Reference}} \right] / \left( \frac{^{13}\text{C}}{^{12}\text{C}} \right)_{\text{Reference}} \quad (1)$$

The magnitude of the degradation-induced isotope fractionation depends on different factors, which can make isotope ratios of specific elements particularly attractive to observe degradation-induced isotope fractionation. To this end, first, an element needs to be directly involved in the

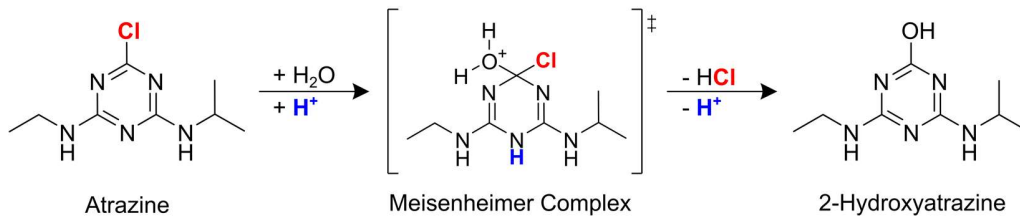
(bio)chemical reaction. For example, a carbon isotope effect would be quite generally expected in organic molecules, whereas a chlorine isotope effect would be primarily expected if a C-Cl bond is cleaved. Second, isotope fractionation depends on the underlying kinetic isotope effect (see above), but also on the extent to which this effect is represented in the molecular average isotope fractionation described by the enrichment factor  $\epsilon$  (see below). Atrazine, for example, contains only one chlorine atom but eight carbon and five nitrogen atoms. Hence, chlorine isotope effects at the reacting position are fully represented in the molecular average, whereas position-specific carbon and nitrogen isotope effects are diluted by non-reacting atoms<sup>14, 15</sup>.

Most of the publications studying the chemical mechanisms of abiotic and microbial atrazine degradation have focused on the analysis of carbon ( $^{13}\text{C}/^{12}\text{C}$ ) and nitrogen ( $^{15}\text{N}/^{14}\text{N}$ ) isotope fractionation. Thereby,  $\epsilon$ -values in the range of -5.4 ‰ to -1.8 ‰ for carbon and -1.9 ‰ to 3.3 ‰ for nitrogen were observed<sup>9, 10, 16, 17</sup>. Chlorine isotope effects for microbial atrazine degradation were so far not reported due to analytical challenges<sup>18</sup>: Until recently<sup>19, 20</sup>, suitable methods were not available for chlorine isotope analysis of atrazine. However, from the magnitude of chlorine isotope effects observed for dechlorination of trichloroethenes (-5.7 ‰ to -3.3 ‰, where intrinsic isotope effects are diluted by a factor of three<sup>21</sup>), very large chlorine enrichment factors  $\epsilon_{\text{Cl}}$  (-8 ‰ to -10 ‰ or even larger) could potentially occur for a C-Cl bond cleavage in atrazine. For example, enzymatic hydrolysis of the structural homologue ametryn (atrazine structure with a -SCH<sub>3</sub> instead of a -Cl group) yielded a sulfur isotope enrichment factor  $\epsilon_{\text{S}}$  of -14.7 ‰  $\pm$  1.0 ‰<sup>17</sup>. If the cleavage of carbon-chlorine bonds is involved in the rate-determining step of a (bio)transformation, chlorine isotope effects could, therefore, enable a particularly sensitive detection of natural transformation processes by compound-specific (i.e., molecular average) isotope analysis.

The measurement of chlorine isotope fractionation is attractive for yet another reason – multiple element isotope analysis bears potential for a better distinction of sources and transformation pathways. From isotope analysis of one element alone, it is difficult to distinguish sources of a particular compound, or competing transformation pathways that may lead to metabolites of different toxicity<sup>15</sup>. For example, two different microbial transformation pathways can lead to the degradation of atrazine in the environment. Hydrolysis forms the nontoxic dehalogenated product 2-hydroxyatrazine (HAT) whereas oxidative dealkylation degrades atrazine to the still herbicidal

products desethyl- (DEA) or desisopropylatrazine (DIA)<sup>22, 23</sup>. Prominent examples for microorganisms catalyzing these pathways are *Arthrobacter aurescens* TC1 and *Rhodococcus* sp. NI86/21 (see Figure 1). *A. aurescens* TC1 was directly isolated from an atrazine-contaminated soil<sup>24</sup>. By expressing the enzyme TrzN, it is capable of performing hydrolysis of atrazine<sup>24, 25</sup>. *Rhodococcus* sp. NI86/21 uses a cytochrome P450 system for catalyzing oxidative dealkylation of atrazine<sup>26</sup>.

***Arthrobacter aurescens* TC1 (TrzN): Hydrolysis**



***Rhodococcus* sp. NI86/21 (Cytochrome P450): Oxidative Dealkylation**

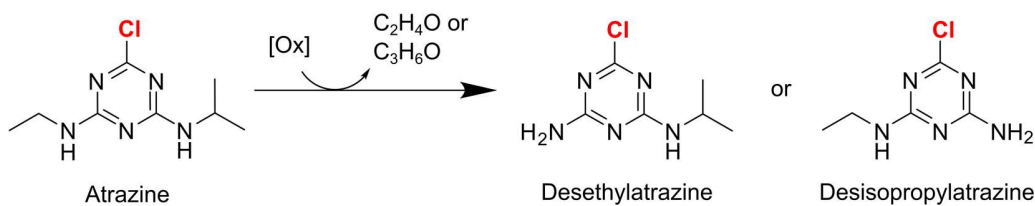


**Figure 1.** Microbial degradation of atrazine by *Arthrobacter aurescens* TC1 and *Rhodococcus* sp. NI86/21 (adapted from Meyer et al.<sup>9</sup> and Meyer & Elsner<sup>10</sup>).

For these two pathways, carbon isotope fractionation was very similar, but significant differences were observed in nitrogen isotope effects<sup>9, 10, 16, 17</sup>. Plotting the changes of isotope ratios of these two elements relative to each other results in the regression slope  $\Lambda$  for carbon and nitrogen<sup>27, 28</sup>

$$\Lambda_{C/N} = \Delta\delta^{15}\text{N} / \Delta\delta^{13}\text{C} \approx \epsilon_{\text{N}} / \epsilon_{\text{C}} \quad (2)$$

Hence, dual element (C, N) isotope trends for oxidative dealkylation of atrazine with *Rhodococcus* sp. NI86/21 ( $\Lambda^{Rhodo}_{C/N} = 0.4 \pm 0.1$ )<sup>16</sup> were significantly different compared to hydrolysis with *A. aurescens* TC1 ( $\Lambda^{Arthro}_{C/N} = -0.6 \pm 0.1$ )<sup>9</sup> offering an opportunity to distinguish atrazine degradation pathways in the field. However, in environmental assessments it is advantageous to have isotopic information of as many elements as possible in order to distinguish

degradation pathways and sources at the same time<sup>29-31</sup>. Therefore, information from a third element, chlorine, would be highly valuable. Also on the mechanistic end, information gained from a change in the chlorine isotope value could lead to a more reliable differentiation of transformation pathways and contribute to a better mechanistic understanding of the underlying chemical reaction<sup>31</sup>. Along these lines, triple element (3D) isotope analysis was already accomplished for chlorinated alkanes<sup>31, 32</sup> and alkenes<sup>33, 34</sup>.

Until now, however, compound-specific chlorine isotope analysis has not been accessible so that chlorine isotope ratio changes for hydrolysis of atrazine have only been analyzed in abiotic systems or via computational calculations<sup>35, 36</sup>. For oxidative dealkylation, chlorine isotope effects have, so far, not been studied. Recently a GC-qMS method for chlorine isotope analysis of atrazine has been brought forward<sup>20</sup> which offers the opportunity to enable deeper mechanistic insights into its transformation processes. Therefore, our objective was to analyze carbon, nitrogen and chlorine isotope effects associated with the biodegradation of atrazine via hydrolysis with *A. aurescens* TC1 and via oxidative dealkylation with *Rhodococcus* sp. NI86/21. In addition, we computationally predicted the chlorine isotope effect associated with hydrolysis and oxidative dealkylation for comparison. Further, we evaluated whether the additional information from chlorine isotope fractionation is a particularly sensitive indicator for transformation processes and whether it can confirm previously proposed mechanisms of different pathways. With this study, we bring forward information about degradation-induced chlorine isotope fractionation of atrazine as a basis to apply triple element (3D) isotope analysis in environmental assessments.

## MATERIAL & METHODS

**Bacterial strains and cultivation.** *A. aurescens* strain TC1 was grown in mineral salt medium supplemented with approx. 20 mg/L of atrazine according to the protocol of Meyer et al.<sup>9</sup> Likewise, *Rhodococcus* sp. strain NI86/21 was cultivated in autoclaved nutrient broth (8 g/L, Difco<sup>TM</sup>) with approx. 20 mg/L of atrazine according to the protocol of Meyer et al.<sup>16</sup>. In the late-exponential growth phase the strains were harvested via centrifugation (4000 rpm, 15 min). For the start of the degradation experiments, cell pellets of each strain were transferred to 400 mL fresh media and atrazine was added to achieve a starting concentration of 20 mg/L. All experiments were performed in triplicate at 21 °C on a shaker at 150 rpm. Control experiments, which were performed without the bacterial strains, did not show any degradation of atrazine.

**Concentration measurements via HPLC.** The process of atrazine degradation was monitored by concentration measurements. For analysis, 1 mL samples were taken and filtered through a 0.22  $\mu\text{m}$  filter. Atrazine and its degradation products were directly analyzed using a Shimadzu UHPLC-20A system, which was equipped with an ODS column 30 (Ultracarb 5  $\mu\text{M}$ , 150  $\times$  4.6 mm, Phenomenex). After sample injection (10  $\mu\text{L}$ ) an adequate gradient program (see SI) was used for compound separation. The oven temperature was set to 45  $^{\circ}\text{C}$  and the compounds were detected by their UV absorbance at 222 nm. Quantitation was performed by the software “Lab Solutions” based on internal calibration curves.

**Preparation of samples for isotope analysis.** According to the protocol of Meyer et al.<sup>9</sup> between 10 and 260 mL of sample were taken for isotope analysis of atrazine at every sampling event. After centrifugation (15 min, 4000 rpm) the supernatant was collected in a new vial. Subsequently, samples were extracted by adding dichloromethane (5-130 mL) and shaking the vial for at least 20 min. The sample extracts were dried at room temperature under the fume hood. Afterwards, the dried extracts were dissolved in ethyl acetate to a final atrazine concentration of approx. 200 mg/L.

**Isotope analysis of carbon and nitrogen.** The protocol for isotope analysis of carbon and nitrogen was adapted from the studies of Meyer et al.<sup>9, 16</sup>. A TRACE GC Ultra gas chromatograph hyphenated with a GC-III combustion interface and coupled to a Finnigan MAT253 isotope ratio mass spectrometer (GC-C-IRMS, all Thermo Fisher Scientific) was used. Each sample was analyzed in triplicate. Sample injection (2-3  $\mu\text{L}$ ) was performed by a Combi-PAL autosampler (CTC Analysis). The injector had a constant temperature of 220  $^{\circ}\text{C}$ , was equipped with an “A” type packed liner for large volume injections (GL Sciences) and was operated for 1 min in splitless and then in split mode (split ratio 1:10) with a flow rate of 1.4 mL/min. For peak separation, the GC oven was equipped with a DB-5 MS column (30 m  $\times$  0.25 mm, 1  $\mu\text{m}$  film thickness, Agilent). The temperature program of the oven started at 65  $^{\circ}\text{C}$  (held for 1 min), ramped at 20  $^{\circ}\text{C}/\text{min}$  to 180  $^{\circ}\text{C}$  (held for 10 min) and ramped again at 15  $^{\circ}\text{C}/\text{min}$  to 230  $^{\circ}\text{C}$  (held for 8 min). In the combustion interface, a GC Isolink II reactor (Thermo Fisher Scientific) was installed, which was operated at a temperature of 1000  $^{\circ}\text{C}$ . After combustion of the analytes to  $\text{CO}_2$  and subsequent reduction of any nitrogen oxides, the compounds were analyzed as  $\text{CO}_2$  for carbon and  $\text{N}_2$  for nitrogen isotope measurements. Three pulse of  $\text{CO}_2$  or  $\text{N}_2$ , respectively, were introduced at the

beginning and at the end of each run as monitoring gas. Beforehand, these monitoring gases were calibrated against RM8563 (CO<sub>2</sub>) and NSVEC (N<sub>2</sub>), which were supplied by the International Atomic Energy Agency (IAEA). The analytical uncertainty 2σ was ±0.5 ‰ for carbon isotope values and ±1.0 ‰ for nitrogen isotope values.

**Isotope analysis of chlorine.** For chlorine isotope analysis of atrazine, a 7890A gas chromatograph coupled to a 5975C quadrupole mass spectrometer (GC-qMS, both Agilent) was used. Sample injection (2 μL) was performed by a Pal Combi-xt autosampler (CTC Analysis). For the injector and the GC oven, the same parameters as for carbon and nitrogen isotope analysis were used with the exception that a different liner type, a “FocusLiner” (SGE), was used. The ion source had a constant temperature of 230 °C and the quadrupole of 150 °C. Prior to sample analysis, the method of Ponsin et al.<sup>20</sup> was tested and optimized for our instrument (see details in SI). Chlorine isotope ratios were evaluated by monitoring the mass-to-charge ratio *m/z* of 202/200. Standards and samples were measured ten times each and uncertainties were reported as standard deviation *s*. Results were only evaluated if the peak areas of samples were inside a defined linearity range (peak area of 1.2 × 10<sup>8</sup> – 3.0 × 10<sup>8</sup> for *m/z* 200). Inside the linearity range, the determined precision of the method is associated with a maximal deviation of ±1.1 ‰. For analysis, the samples were diluted with ethyl acetate to a final concentration of approx. 75 mg/L and measured with a dwell time of 100 ms. Correction of the chlorine isotope values relative to Standard Mean Ocean Chloride (SMOC) was performed by an external two-point calibration with characterized standards of atrazine (Atr #4 δ<sup>37</sup>Cl = -0.89 ‰ and Atr #11 δ<sup>37</sup>Cl = +3.59 ‰)<sup>37</sup>. To this end, the standards were measured at the beginning, in between and at the end of each sequence.

**Evaluation of stable isotope fractionation.** Determination of isotope enrichment factors ε was achieved by the Rayleigh equation, which describes the gradual enrichment of the residual substrate fraction *f* with molecules containing heavy isotopes, as expressed by isotope values according to eq. 1<sup>15,38</sup>. For example, for chlorine:

$$\ln [ (\delta^{37}\text{Cl} + 1) / (\delta^{37}\text{Cl}_0 + 1) ] = \epsilon_{\text{Cl}} \cdot \ln f \quad (3)$$

Here δ<sup>37</sup>Cl<sub>0</sub> refers to the chlorine isotope value at the starting point (*t* = 0) of an experiment. Regression slopes Λ of dual element isotope plots were obtained by plotting isotope ratios of two different elements against each other, e.g. carbon vs. nitrogen (see eq. 2). The uncertainties of the



calculated  $\epsilon$ -values and  $\Lambda$ -values are reported as 95 % confidence intervals (CI). Furthermore, (apparent) kinetic isotope values, (A)KIE<sub>Cl</sub>, that express the ratio of reaction rates <sup>35</sup>k and <sup>37</sup>k of heavy and light isotopologues, respectively,

$$\text{KIE}_{\text{Cl}} = {}^{35}\text{k} / {}^{37}\text{k} \quad (4)$$

were calculated according to Elsner et al.<sup>15</sup> by converting  $\epsilon_{\text{Cl}}$ -values into (A)KIE<sub>Cl</sub> and taking into account that atrazine contains only one chlorine atom ( $n = 1$ ):

$$(\text{A})\text{KIE}_{\text{Cl}} = 1 / (n \times \epsilon_{\text{Cl}} + 1) \quad (5)$$

**Prediction of chlorine kinetic isotope effects during oxidative dealkylation and hydrolysis of atrazine.** In the computational part of the study, we considered hydrogen atom transfer and hydride transfer taking place at the  $\alpha$ -position of the ethyl side chain of the atrazine molecule in the oxidative dealkylation reaction promoted by permanganate and the hydronium ion, respectively. Furthermore, we considered hydrolysis under acidic/enzymatic, neutral and alkaline conditions. All molecular structures and analytical vibrational frequencies for involved reactant complexes and transition states were taken from a previous study<sup>16</sup>. Chlorine kinetic isotope effects were calculated using the complete Bigeleisen equation<sup>39</sup> implemented in the ISOEFF program<sup>40</sup> at 300 K. The tunneling contributions to the overall kinetic isotope effect were omitted.

## RESULTS & DISCUSSION

**Observation of normal chlorine isotope effects in biotic hydrolysis and oxidative dealkylation.** Atrazine degradation by *A. aurescens* TC1 resulted in the metabolite 2-hydroxyatrazine, whereas the metabolites DEA and DIA were observed for *Rhodococcus* sp. NI86/21 (see Figure S4 and S5 in the SI). Detection of these expected degradation products (Figure 1) demonstrates that hydrolysis and oxidative dealkylation were the underlying biochemical reactions during atrazine degradation, respectively. In both biodegradation experiments – biotic hydrolysis with *A. aurescens* TC1 and oxidative dealkylation with *Rhodococcus* sp. NI86/21 – normal chlorine isotope fractionation was observed (see Figure 2A). In the three replicates of hydrolytic degradation by *A. aurescens* TC1 90 %, 90 % and 60 % transformation of atrazine was reached after approx. 26 h, respectively (see SI, Figure S4). Evaluation of  $\delta^{37}\text{Cl}$  values during biotic hydrolysis according to Equation 3 resulted in a small

normal isotope effect of  $\epsilon_{\text{Cl}} = -1.4 \pm 0.6 \text{ ‰}$ . In oxidative dealkylation with *Rhodococcus* sp. NI86/21 approx. 90 % degradation was reached after approx. 186 h in all three replicates (see SI, Figure S5). Evaluation of changes in chlorine isotope ratios resulted in a surprisingly large normal isotope effect of  $\epsilon_{\text{Cl}} = -4.3 \pm 1.8 \text{ ‰}$  considering that the C-Cl bond is not broken during the reaction (see Figure 1). In a next step, carbon and nitrogen isotope effects were therefore analyzed to confirm whether the same reactions mechanisms are at work as observed in previous studies<sup>9, 16</sup>.

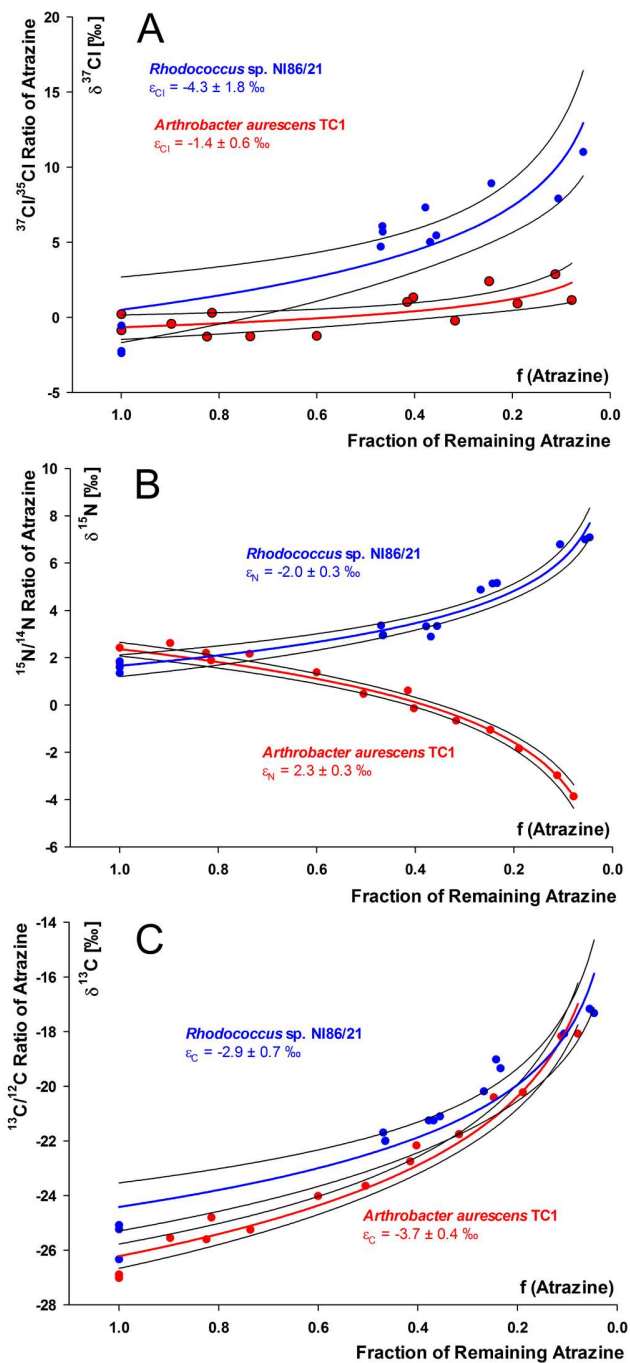


**Figure 2.** Isotope fractionation of (A) chlorine, (B) nitrogen and (C) carbon during microbial degradation of atrazine by *A. aureescens* TC1 (red) and *Rhodococcus* sp. NI86/21 (blue) and corresponding enrichment factors  $\epsilon$  evaluated according to eq. 3. (The 95 % confidence intervals are given as values and as black lines).

**Observed carbon and nitrogen isotope fractionation is consistent with previous studies.**

Carbon and nitrogen isotope fractionation for atrazine degradation by *A. aurescens* TC1 and *Rhodococcus* sp. NI86/21 was consistent with previous studies: Both experiments showed significant changes in isotope ratios (see Figure 2B and C). For hydrolysis with *A. aurescens* TC1, an inverse nitrogen isotope effect ( $\epsilon_N = 2.3 \pm 0.3 \text{ ‰}$ ) and a normal carbon isotope effect ( $\epsilon_C = -3.7 \pm 0.4 \text{ ‰}$ ) were observed, which were slightly smaller compared to the results of a former publication of Meyer et al. ( $\epsilon_N = 3.3 \pm 0.4 \text{ ‰}$ ,  $\epsilon_C = -5.4 \pm 0.6 \text{ ‰}$ )<sup>9</sup>, but gave the same dual element isotope plot ( $\Lambda^{Arthro}_{C/N} = -0.6 \pm 0.1$ ) confirming that the same mechanism was at work (see Figure 3A).

Oxidative dealkylation of atrazine with *Rhodococcus* sp. NI86/21 resulted in a normal nitrogen isotope effect of  $\epsilon_N = -2.0 \pm 0.3 \text{ ‰}$  and a normal carbon isotope effect of  $\epsilon_C = -2.9 \pm 0.7 \text{ ‰}$ . These  $\epsilon$ -values are similar to those published by Meyer & Elsner<sup>10</sup> ( $\epsilon_N = -1.5 \pm 0.3 \text{ ‰}$ ,  $\epsilon_C = -4.0 \pm 0.2 \text{ ‰}$ ) and Meyer et al.<sup>16</sup> ( $\epsilon_N = -1.4 \pm 0.3 \text{ ‰}$ ,  $\epsilon_C = -3.8 \pm 0.2 \text{ ‰}$ ). The slightly more pronounced nitrogen isotope fractionation in this study can probably be attributed to the fact that oxidation was primarily observed at the C-H bond adjacent to the nitrogen atom ( $\alpha$ -position of the ethyl or isopropyl group)<sup>16</sup>. In the study of Meyer et al.<sup>16</sup> 52 % of the oxidation was observed at the  $\alpha$ -position and 48 % at the  $\beta$ -position of the ethyl or isopropyl group which resulted in a smaller nitrogen isotope fractionation effect. The obtained regression slope of  $\Lambda^{Rhodo}_{C/N} = 0.7 \pm 0.1$  in this study is slightly larger than the previously reported regression slopes ( $\Lambda^{Rhodo}_{C/N} = 0.4 \pm 0.1$ )<sup>10, 16</sup> which may again be explained by the small difference in average nitrogen isotope effects. Also here, however, the similar dual element isotope trend confirms that in this study atrazine was transformed by the same mechanism as in Meyer et al.<sup>16</sup> leading to the observed oxidative dealkylation products by *Rhodococcus* sp. NI86/21.

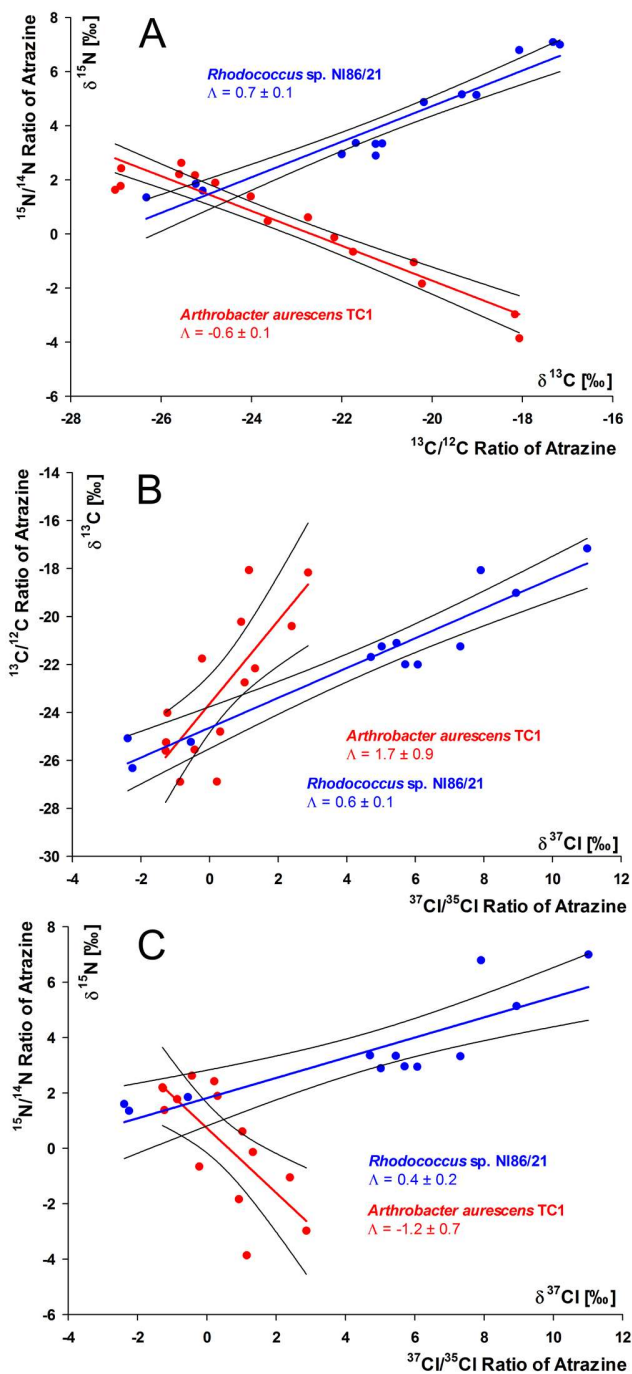


**Figure 3.** Isotope effects in microbial degradation of atrazine by *A. aureescens* TC1 (red) and *Rhodococcus* sp. NI86/21 (blue) resulting in dual element isotope plots. (The 95 % confidence intervals are given as values and as black lines next to the regression slopes). (A) Regression slopes of nitrogen and carbon isotope values ( $\Lambda_{\text{C/N}}$ ). (B) Regression slopes of chlorine and carbon isotope values ( $\Lambda_{\text{Cl/C}}$ ). (C) Regression slopes of chlorine and nitrogen isotope values ( $\Lambda_{\text{Cl/N}}$ ).

**Multi-element isotope approach.** Results of chlorine isotope analysis were combined with data for carbon and nitrogen isotope measurements in dual element isotope plots (see Figure 3B and C). For hydrolysis with *A. aurescens* TC1 regression slopes of  $\Lambda^{Arthro}_{Cl/C} = 1.7 \pm 0.9$  and  $\Lambda^{Arthro}_{Cl/N} = -1.2 \pm 0.7$  were obtained. Oxidative dealkylation by *Rhodococcus* sp. NI86/21 resulted in regression slopes of  $\Lambda^{Rhodo}_{Cl/C} = 0.6 \pm 0.1$  and  $\Lambda^{Rhodo}_{Cl/N} = 0.4 \pm 0.2$ . Since the dual element isotope plots of chlorine and carbon and of chlorine and nitrogen provide significantly different regression slopes for the respective elements, they can provide an additional line of evidence to differentiate the two degradation mechanisms of atrazine from each other.

**Surprising mechanistic evidence from chlorine isotope effects.** For degradation with *A. aurescens* TC1, rather small chlorine isotope fractionation was observed ( $\epsilon_{Cl} = -1.4 \pm 0.6 \text{ ‰}$ ) despite the fact that the chlorine is cleaved off during hydrolysis (see Figure 1). For oxidative dealkylation with *Rhodococcus* sp. NI86/21, the chlorine is not cleaved off (see Figure 1), therefore, no or just a small chlorine isotope effect was expected. However, here more pronounced chlorine isotope fractionation was observed ( $\epsilon_{Cl} = -4.3 \pm 1.8 \text{ ‰}$ ).

The corresponding apparent kinetic isotope effects ( $AKIE_{Cl}$ , see Table 1) were compared to the  $AKIE_{Cl}$  values of other studies focusing on the same degradation mechanisms. In addition, the  $AKIE_{Cl}$  values were compared to the theoretical maximum Streitwieser Limit associated with the cleavage of a C-Cl bond ( $KIE_{Cl} = 1.02$ )<sup>41-43</sup> and to the predictions of computational calculations (Table 2).

**Table 1.**  $AKIE_{Cl}$  values associated with atrazine degradation.

Mechanism	$AKIE_{Cl}$	Study
<b>Experimental Data</b>		
abiotic alkaline hydrolysis (21 °C)	$1.0069 \pm 0.0005$	Dybala-Defratyka et al. <sup>35</sup>
abiotic alkaline hydrolysis (50 °C),	$1.0009 \pm 0.0006$	Grzybkowska et al. <sup>36</sup>
microbial hydrolysis ( <i>A. aurescens</i> TC1)	$1.0014 \pm 0.0006^*$	this study
microbial dealkylation ( <i>Rhodococcus</i> sp. NI86/21)	$1.0043 \pm 0.0018^*$	this study
<b>Computational Data</b>		
abiotic acidic hydrolysis	range of 1.0002 to 1.0011	Grzybkowska et al. <sup>36</sup>
abiotic alkaline hydrolysis	range of 1.0003 to 1.0014	Grzybkowska et al. <sup>36</sup>
enzymatic hydrolysis	range of 0.9996 to 1.0003	Szatkowski et al. <sup>44</sup>
abiotic dealkylation (hydrogen atom transfer by $MnO_4^-$ )	0.9999	this study
abiotic dealkylation (hydride transfer by $H_3O^+$ )	0.9997	this study

---

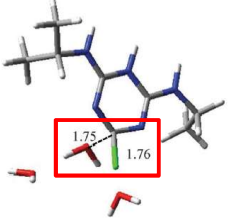
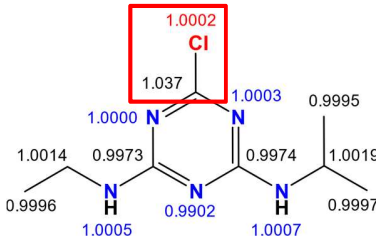
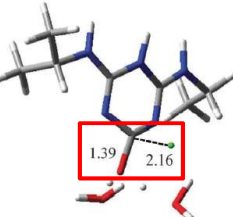
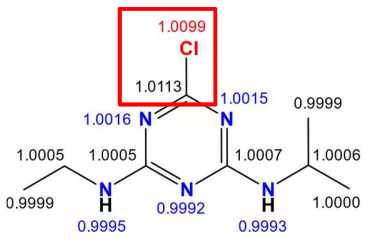
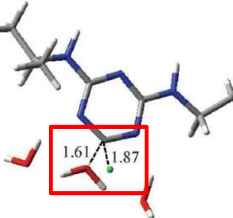
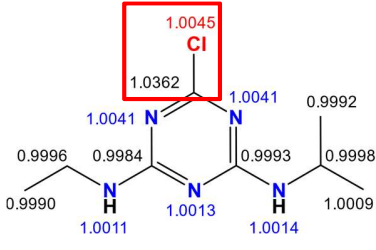
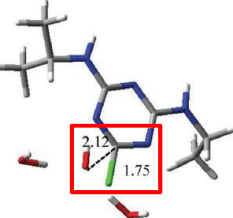
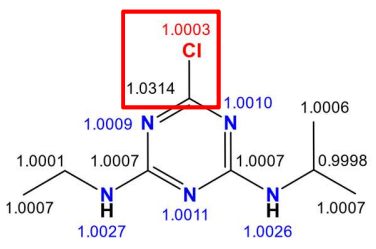
\* calculated according to eq. 5

For microbial hydrolysis of atrazine an experimental  $AKIE^{Arthro}_{Cl}$  value of  $1.0014 \pm 0.0006$  was calculated (see Table 1). Dybala-Defratyka et al.<sup>35</sup> reported a more pronounced  $AKIE^{alk.hydrol.}_{Cl}$  value of  $1.0069 \pm 0.0005$  (see Table 1). However, that study<sup>35</sup> was conducted in an abiotic alkaline solution at 21 °C so that another hydrolysis pathway was involved. Newer data reported a much smaller value of  $AKIE^{alk.hydrol.}_{Cl} = 1.0009 \pm 0.0006$ <sup>36</sup> for the same alkaline hydrolysis at 50 °C. Later on it was confirmed that abiotic alkaline hydrolysis performed earlier at 21 °C resembles rather neutral than alkaline conditions<sup>36</sup>. Table 2 illustrates the different computed mechanisms that lie at the heart of the computational predictions. It shows the different mechanistic routes between the alkaline (substitution of Cl without protonation of the atrazine ring) and the acidic/enzymatic pathway characterized in Meyer et al.<sup>9</sup> (substitution of Cl with protonation of the atrazine ring) including different possible transition states. As a general rule, chlorine isotope effects are determined by the C-Cl bond order in the transition state (the lower the bond order, the greater the changes in bonding, the greater the chlorine isotope effect). Previously performed computations<sup>36</sup> and computations of this study mimicking alkaline, acidic, and neutral conditions indicated that the largest  $AKIE_{Cl}$  should be expected under neutral conditions (except for transition state 2 of acidic/enzymatic hydrolysis). Under neutral conditions the C-Cl bond is elongated leading to a transition state geometry which differs substantially from hydrolysis reactions promoted either by alkaline or acidic conditions (see Table 2). However, hydrolysis at neutral pH is too slow to be of relevance. Computational calculations taking into account the transition state structures at a molecular level predicted  $AKIE_{Cl}$  values ranging from 0.9996 to 1.0014 for alkaline, acidic and enzymatic hydrolysis (see Table 1 and 2)<sup>36, 44</sup>. Hence, on the mechanistic level, the computational studies predict that the formation of a Meisenheimer complex rather than the subsequent C-Cl bond cleavage is the rate-determining step during the nucleophilic aromatic substitution reaction catalyzed by TrzN<sup>36, 44</sup>. In both abiotic pathways the C-Cl bond at the transition state of the rate determining step is almost intact giving rise to very small  $AKIE_{Cl}$  (the computed bond orders for both alkaline and acidic hydrolysis are the same and equal to 1.03, see also Table 2). In this study, we therefore observed a similarly small  $AKIE^{Arthro}_{Cl}$  value for enzymatic hydrolysis in *A. aurescens* TC1 which resembles acid-catalyzed hydrolysis rather than alkaline hydrolysis<sup>9</sup>. Hence, a consistent picture emerges that different hydrolytic pathways give

rise to experimental  $AKIE_{Cl}$  values much lower than the Streitwieser Limit of  $1.02^{41-43}$  indicating that the chlorine isotope effect is masked in all cases and that the C-Cl bond cleavage is not the rate-determining step. Interestingly, this is in contrast to ametryn hydrolysis where strong sulphur isotope effects were observed in enzymatic hydrolysis by TrzN<sup>17</sup>. In conclusion, since chlorine isotope effects were found to be masked, information from chlorine isotope analysis alone would not be enough to differentiate the different reaction mechanisms. This illustrates the importance of analyzing more than one element for mechanistic differentiation.



- 1 **Table 2.** Mechanisms and transition states of acidic/enzymatic, neutral and alkaline hydrolysis and corresponding calculated and  
 2 measured isotope effects.

Mechanism	Calculated Transition State <sup>a</sup>	Calculated Isotope Effect (position-specific and compound average AKIE values)	Measured Isotope Effect
Acidic/Enzymatic Hydrolysis (Transition State 1)	 <p><b>C-Cl Bond Order: 1.03</b></p>	 <p><b>Compound average:</b>  <b>AKIE<sub>Cl</sub> = 1.0002</b>        AKIE<sub>N</sub> = 0.9983        AKIE<sub>C</sub> = 1.0042</p>	<p><b>Compound average:</b>        AKIE<sub>Cl</sub> = 1.0014 ± 0.0006<sup>b</sup>        AKIE<sub>N</sub> = 0.9886 ± 0.0015<sup>b</sup>        AKIE<sub>C</sub> = 1.0271 ± 0.0034<sup>b</sup></p>
Acidic/Enzymatic Hydrolysis (Transition State 2)	 <p><b>C-Cl Bond Order: 0.55</b></p>	 <p><b>Compound average:</b>  <b>AKIE<sub>Cl</sub> = 1.0099</b>        AKIE<sub>N</sub> = 1.0002        AKIE<sub>C</sub> = 1.0017</p>	-
Neutral Hydrolysis	 <p><b>C-Cl Bond Order: 0.87</b></p>	 <p><b>Compound average:</b>  <b>AKIE<sub>Cl</sub> = 1.0045</b>        AKIE<sub>N</sub> = 1.0024        AKIE<sub>C</sub> = 1.0041</p>	-
Alkaline Hydrolysis	 <p><b>C-Cl Bond Order: 1.03</b></p>	 <p><b>Compound average:</b>  <b>AKIE<sub>Cl</sub> = 1.0003</b>        AKIE<sub>N</sub> = 1.0017        AKIE<sub>C</sub> = 1.0043</p>	<p><b>Compound average:</b>        AKIE<sub>Cl</sub> = 1.0009 ± 0.0006<sup>a</sup>        AKIE<sub>N</sub> = 1.001 ± 0.000<sup>c</sup>        AKIE<sub>C</sub> = 1.031 ± 0.003<sup>c</sup></p>

3 <sup>a</sup> taken from Grzybkowska et al.<sup>36</sup>, <sup>b</sup> calculated according to eq. 5 (main manuscript) with n = 5 for N and n = 8 for C, <sup>c</sup> taken from Meyer et al.<sup>9</sup>

5 For oxidative dealkylation, so far, no chlorine isotope effects were reported. Regarding the  
6 reaction mechanism, Meyer et al.<sup>16</sup> concluded that oxidative dealkylation of atrazine with  
7 *Rhodococcus* sp. NI86/21 is initiated by hydrogen atom transfer based on the observed product  
8 distribution and the carbon and nitrogen isotope effects. Hydrogen atom transfer leads directly to  
9 a homolytic cleavage of the C-H bond adjacent to the nitrogen atom ( $\alpha$ -position of the ethyl or  
10 isopropyl group) producing a relative unstable 1,1-aminoalcohol which is then further transformed  
11 to DEA or DIA<sup>16</sup>. In parallel, two additional products could be detected which were formed by  
12 oxidation of the C-H bond in the  $\beta$ -position of the ethyl or isopropyl group. For this mechanistic  
13 pathway, chlorine isotope effects would be expected to be rather small since the chlorine is not  
14 involved in the reaction steps. The closed mass balance of the concentration analysis (see  
15 Figure S5 in the SI) of this study and the results of product distribution of Meyer et al.<sup>16</sup> also  
16 indicate that there is no C-Cl bond cleavage taking place since corresponding hydrolysis products  
17 were not detected. Furthermore, our computations for hydrogen atom transfer at a catalytic center  
18 mimicking cytochrome P450 predicted no chlorine isotope effect ( $AKIE^{\text{hydro.atom trans.}_{Cl}} = 0.9999$ ,  
19 see Table 1). Hydride transfer promoted by the hydronium ion also resulted in no chlorine isotope  
20 effect ( $AKIE^{\text{hydride trans.}_{Cl}} = 0.9997$ , see Table 1). At previously located transition state structures  
21 for these two reactions<sup>16</sup> the carbon-chlorine bond remains intact and no stretching of this bond is  
22 involved in the reaction coordinate (hydrogen transfer) mode. The observed more pronounced  
23  $AKIE^{\text{Rhodo}_{Cl}}$  value of  $1.0043 \pm 0.0018$  in this study (see Table 1) could, therefore, be indicative of  
24 isotope effects caused by enzymatic interactions. Meyer et al.<sup>16</sup> proposed that for oxidative  
25 dealkylation no selectivity itself is observed, however, the preferred oxidation of the  $\alpha$ -position  
26 over the  $\beta$ -position could be explained by steric factors of the catalyzing enzyme which could have  
27 an influence on the transformation pathway. Thus, the sensitive chlorine isotope effect, which is  
28 observed even though the C-Cl bond is not cleaved during degradation, can be interpreted as an  
29 indicator that non-covalent interactions between the cytochrome P450 complex and the chlorine  
30 cause significant chlorine isotope fractionation<sup>45</sup>.

## 31 CONCLUSION

32 Since atrazine is frequently detected in groundwater systems, major efforts should be put into  
33 understanding its environmental fate. We provide an approach to 3D-isotope (C, N, Cl) analysis  
34 of atrazine and explored isotope fractionation in different transformation pathways. Together, this

35 provides the basis to more confidently assess sources and degradation of atrazine in the  
36 environment. Specifically, we demonstrated that pronounced changes in chlorine isotope values  
37 are not an indicator of microbial hydrolysis (as one might have expected without knowledge of  
38 our experimental data), but – surprisingly – rather of oxidative dealkylation. Therefore, although  
39 trends are different than expected, they can nonetheless be used for a more confident identification  
40 of different sources and transformation pathways in field samples. Regarding the sensitivity of  
41 chlorine isotope effects, our study demonstrates the importance of performing controlled  
42 laboratory experiments before applying the approach in the field. Specifically, in other cases  
43 chlorine isotope fractionation can be much more pronounced than observed for atrazine in this  
44 study. Large chlorine isotope effects were observed in proof-of-principle experiments by Ponsin  
45 et al.<sup>20</sup> studying hydrolytic dechlorination of S-metolachlor, an herbicide containing also only one  
46 chlorine atom. Here preliminary data suggest a large chlorine isotope effect of  $\epsilon_{\text{Cl}} = -9.7 \pm 2.9 \text{ ‰}$   
47 for abiotic alkaline hydrolysis. Therefore, in the case of other substances chlorine isotope effects  
48 can be even more sensitive indicators of degradation provided that the C-Cl bond cleavage occurs  
49 in the rate-determining step of a reaction. Further, gaining deeper insights into these chemical  
50 processes is the basis for understanding the biotic catalysis of organic micropollutant degradation.  
51 This, in turn, is essential for identifying and developing optimized strategies for micropollutant  
52 removal in order to make successful bioremediation possible.

### 53 CONFLICT OF INTEREST

54 There are no conflicts to declare.

### 55 ACKNOWLEDGMENT

56 This work was supported by the Swiss National Science Foundation (SNSF, Grant  
57 CRSII2\_141805), the German Israeli Foundation for Scientific Research and Development (GIF,  
58 Grant I-251-307.4-2013) and the National Science Center in Poland (Sonata BIS grant UMO-  
59 2014/14/E/ST4/00041). We thank PLGrid Infrastructure (Poland) for computer resources and  
60 Armin Meyer for his advice regarding the microbial degradation experiments.

### 61 REFERENCES

- 62 1. H. Gysin and E. Knusli, Chemistry and herbicidal properties of triazine derivatives, *Adv.*  
63 *in Pest Control Res.*, 1960, **3**, 289-353.

- 64 2. EPA, Pesticides Industry Sales and Usage: 2008–2012 Market Estimates, *US*  
65 *Environmental Protection Agency, Washington (DC)*, 2017.
- 66 3. European Commission, Commission decision of 10 March 2004 concerning the non-  
67 inclusion of atrazine in Annex I to Council Directive 91/414/EEC and the withdrawal of  
68 authorisations for plant protection products containing this active substance., *Official*  
69 *Journal of the European Union*, 2004, **78**, 53-55.
- 70 4. R. Loos, G. Locoro, S. Comero, S. Contini, D. Schwesig, F. Werres, P. Balsaa, O. Gans,  
71 S. Weiss, L. Blaha, M. Bolchi and B. M. Gawlik, Pan-European survey on the occurrence  
72 of selected polar organic persistent pollutants in ground water, *Water Res.*, 2010, **44**,  
73 4115-4126.
- 74 5. D. Vonberg, J. Vanderborght, N. Cremer, T. Pütz, M. Herbst and H. Vereecken, 20 years  
75 of long-term atrazine monitoring in a shallow aquifer in western Germany, *Water Res.*,  
76 2014, **50**, 294-306.
- 77 6. S. Singh, V. Kumar, A. Chauhan, S. Datta, A. B. Wani, N. Singh and J. Singh, Toxicity,  
78 degradation and analysis of the herbicide atrazine, *Environ. Chem. Lett.*, 2018, **16**, 211-  
79 237.
- 80 7. S. Kern, H. P. Singer, J. Hollender, R. P. Schwarzenbach and K. Fenner, Assessing  
81 exposure to transformation products of soil-applied organic contaminants in surface  
82 water: comparison of model predictions and field data, *Environ. Sci. Technol.*, 2011, **45**,  
83 2833-2841.
- 84 8. C. Moreau-Kervevan and C. Mouvet, Adsorption and desorption of atrazine,  
85 deethylatrazine, and hydroxyatrazine by soil components, *J. Environ. Qual.* , 1998, **27**,  
86 46-53.
- 87 9. A. H. Meyer, H. Penning and M. Elsner, C and N isotope fractionation suggests similar  
88 mechanisms of microbial atrazine transformation despite involvement of different  
89 Enzymes (AtzA and TrzN), *Environ. Sci. Technol.*, 2009, **43**, 8079-8085.
- 90 10. A. H. Meyer and M. Elsner, <sup>13</sup>C/<sup>12</sup>C and <sup>15</sup>N/<sup>14</sup>N Isotope Analysis To Characterize  
91 Degradation of Atrazine: Evidence from Parent and Daughter Compound Values,  
92 *Environ. Sci. Technol.*, 2013, **47**, 6884-6891.
- 93 11. A. H. Meyer, H. Penning, H. Lowag and M. Elsner, Precise and accurate compound  
94 specific carbon and nitrogen isotope analysis of atrazine: critical role of combustion oven  
95 conditions, *Environ. Sci. Technol.*, 2008, **42**, 7757-7763.
- 96 12. S. Reinnicke, D. Juchelka, S. Steinbeiss, A. H. Meyer, A. Hilkert and M. Elsner, Gas  
97 chromatography-isotope ratio mass spectrometry (GC-IRMS) of recalcitrant target  
98 compounds: performance of different combustion reactors and strategies for  
99 standardization, *Rapid. Commun. Mass. Sp.*, 2012, **26**, 1053-1060.
- 100 13. K. Schreglmann, M. Hoeche, S. Steinbeiss, S. Reinnicke and M. Elsner, Carbon and  
101 nitrogen isotope analysis of atrazine and desethylatrazine at sub-microgram per liter  
102 concentrations in groundwater, *Anal. Bioanal. Chem.*, 2013, **405**, 2857-2867.
- 103 14. T. C. Schmidt, L. Zwank, M. Elsner, M. Berg, R. U. Meckenstock and S. B. Haderlein,  
104 Compound-specific stable isotope analysis of organic contaminants in natural  
105 environments: a critical review of the state of the art, prospects, and future challenges,  
106 *Anal. Bioanal. Chem.*, 2004, **378**, 283-300.
- 107 15. M. Elsner, Stable isotope fractionation to investigate natural transformation mechanisms  
108 of organic contaminants: principles, prospects and limitations, *J. Environ. Monit.*, 2010,  
109 **12**, 2005-2031.

- 110 16. A. H. Meyer, A. Dybala-Defratyka, P. J. Alaimo, I. Geronimo, A. D. Sanchez, C. J.  
111 Cramer and M. Elsner, Cytochrome P450-catalyzed dealkylation of atrazine by  
112 *Rhodococcus* sp. strain NI86/21 involves hydrogen atom transfer rather than single  
113 electron transfer, *Dalton Trans.*, 2014, **43**, 12111-12432.
- 114 17. H. K. V. Schürner, J. L. Seffernick, A. Grzybkowska, A. Dybala-Defratyka, L. P.  
115 Wackett and M. Elsner, Characteristic Isotope Fractionation Patterns in s-Triazine  
116 Degradation Have Their Origin in Multiple Protonation Options in the s-Triazine  
117 Hydrolase TrzN, *Environ. Sci. Technol.*, 2015, **49**, 3490-3498.
- 118 18. T. B. Hofstetter and M. Berg, Assessing transformation processes of organic  
119 contaminants by compound-specific stable isotope analysis, *TrAC, Trends Anal. Chem.*,  
120 2011, **30**, 618-627.
- 121 19. J. Renpenning, A. Horst, M. Schmidt and M. Gehre, Online isotope analysis of <sup>37</sup>Cl/<sup>35</sup>Cl  
122 universally applied for semi-volatile organic compounds using GC-MC-ICPMS, *J. Anal.*  
123 *At. Spectrom.*, 2018, **33**, 314-321.
- 124 20. V. Ponsin, C. Torrentó, C. Lihl, M. Elsner and D. Hunkeler, Compound-specific chlorine  
125 isotope analysis of the herbicides atrazine, acetochlor and metolachlor, *Anal. Chem.*,  
126 2019, **91**, 14290-14298.
- 127 21. C. Lihl, L. M. Douglas, S. Franke, A. Pérez-de-Mora, A. H. Meyer, M. Daubmeier, E. A.  
128 Edwards, I. Nijenhuis, B. Sherwood Lollar and M. Elsner, Mechanistic Dichotomy in  
129 Bacterial Trichloroethene Dechlorination Revealed by Carbon and Chlorine Isotope  
130 Effects, *Environ. Sci. Technol.*, 2019, **53**, 4245-4254.
- 131 22. L. E. Erickson, Degradation of atrazine and related s-triazines, *Crit. Rev. Env. Con.*,  
132 1989, **19**, 1-14.
- 133 23. H. M. LeBaron, J. E. McFarland and O. C. Burnside, *The triazine herbicides*, Elsevier,  
134 Oxford, 1 edn., 2008.
- 135 24. L. C. Strong, C. Rosendahl, G. Johnson, M. J. Sadowsky and L. P. Wackett, *Arthrobacter*  
136 *aurescens* TC1 metabolizes diverse s-triazine ring compounds, *Appl. Environ. Microbiol.*,  
137 2002, **68**, 5973-5980.
- 138 25. K. Sajjaphan, N. Shapir, L. P. Wackett, M. Palmer, B. Blackmon, J. Tomkins and M. J.  
139 Sadowsky, *Arthrobacter aurescens* TC1 Atrazine Catabolism Genes *trzN*, *atzB*, and *atzC*  
140 Are Linked on a 160-Kilobase Region and Are Functional in *Escherichia coli*, *Appl.*  
141 *Environ. Microbiol.*, 2004, **70**, 4402-4407.
- 142 26. I. Nagy, F. Compennolle, K. Ghys, J. Vanderleyden and R. De Mot, A single cytochrome  
143 P-450 system is involved in degradation of the herbicides EPTC (S-ethyl  
144 dipropylthiocarbamate) and atrazine by *Rhodococcus* sp. strain NI86/21, *Appl. Environ.*  
145 *Microbiol.*, 1995, **61**, 2056-2060.
- 146 27. M. Elsner, L. Zwank, D. Hunkeler and R. P. Schwarzenbach, A new concept linking  
147 observable stable isotope fractionation to transformation pathways of organic pollutants,  
148 *Environ. Sci. Technol.*, 2005, **39**, 6896-6916.
- 149 28. L. Zwank, M. Berg, M. Elsner, T. C. Schmidt, R. P. Schwarzenbach and S. B. Haderlein,  
150 New evaluation scheme for two-dimensional isotope analysis to decipher biodegradation  
151 processes: application to groundwater contamination by MTBE, *Environ. Sci. Technol.*,  
152 2005, **39**, 1018-1029.
- 153 29. S. Reinnicke, A. Simonsen, S. R. Sørensen, J. Aamand and M. Elsner, C and N Isotope  
154 Fractionation during Biodegradation of the Pesticide Metabolite 2,6-Dichlorobenzamide

- 155 (BAM): Potential for Environmental Assessments, *Environ. Sci. Technol.*, 2012, **46**,  
156 1447-1454.
- 157 30. T. Gilevska, M. Gehre and H. H. Richnow, Multidimensional isotope analysis of carbon,  
158 hydrogen and oxygen as tool for identification of the origin of ibuprofen, *J. Pharm.*  
159 *Biomed. Anal.*, 2015, **115**, 410-417.
- 160 31. J. Palau, O. Shouakar-Stash, S. Hatijah Mortan, R. Yu, M. Rosell, E. Marco-Urrea, D. L.  
161 Freedman, R. Aravena, A. Soler and D. Hunkeler, Hydrogen Isotope Fractionation during  
162 the Biodegradation of 1,2-Dichloroethane: Potential for Pathway Identification Using a  
163 Multi-element (C, Cl, and H) Isotope Approach, *Environ. Sci. Technol.*, 2017, **51**, 10526-  
164 10535.
- 165 32. S. Franke, C. Lihl, J. Renpenning, M. Elsner and I. Nijenhuis, Triple-element compound-  
166 specific stable isotope analysis of 1,2-dichloroethane for characterization of the  
167 underlying dehalogenation reaction in two *Dehalococcoides mccartyi* strains, *FEMS*  
168 *Microbiol. Ecol.*, 2017, **93**, fix137.
- 169 33. T. Kuder, B. M. van Breukelen, M. Vanderford and P. Philp, 3D-CSIA: Carbon,  
170 Chlorine, and Hydrogen Isotope Fractionation in Transformation of TCE to Ethene by a  
171 *Dehalococcoides* Culture, *Environ. Sci. Technol.*, 2013, **47**, 9668-9677.
- 172 34. B. Heckel, K. McNeill and M. Elsner, Chlorinated Ethene Reactivity with Vitamin B12 Is  
173 Governed by Cobalamin Chloroethylcarbanions as Crossroads of Competing Pathways,  
174 *ACS Catal.*, 2018, **8**, 3054-3066.
- 175 35. A. Dybala-Defratyka, L. Szatkowski, R. Kaminski, M. Wujec, A. Siwek and P. Paneth,  
176 Kinetic isotope effects on dehalogenations at an aromatic carbon, *Environ. Sci. Technol.*,  
177 2008, **42**, 7744-7750.
- 178 36. A. Grzybkowska, R. Kaminski and A. Dybala-Defratyka, Theoretical predictions of  
179 isotope effects versus their experimental values for an example of uncatalyzed hydrolysis  
180 of atrazine, *Phys. Chem. Chem. Phys.*, 2014, **16**, 15164-15172.
- 181 37. C. Lihl, J. Renpenning, S. Kümmel, F. Gelman, H. K. V. Schürner, M. Daubmeier, B.  
182 Heckel, A. Melsbach, A. Bernstein, O. Shouakar-Stash, M. Gehre and M. Elsner, Toward  
183 Improved Accuracy in Chlorine Isotope Analysis: Synthesis Routes for In-House  
184 Standards and Characterization via Complementary Mass Spectrometry Methods, *Anal.*  
185 *Chem.*, 2019, **91**, 12290-12297.
- 186 38. D. Hunkeler, R. U. Meckenstock, B. Sherwood Lollar, T. Schmidt, J. Wilson, T. Schmidt  
187 and J. Wilson, *A Guide for Assessing Biodegradation and Source Identification of*  
188 *Organic Ground Water Contaminants using Compound Specific Isotope Analysis (CSIA)*,  
189 O. o. R. a. Development Report PA 600/R-08/148 | December 2008 | [www.epa.gov/ada](http://www.epa.gov/ada),  
190 US EPA, Oklahoma, USA, 2008.
- 191 39. J. Bigeleisen, The relative reaction velocities of isotopic molecules, *J. Chem. Phys.*, 1949,  
192 **17**, 675-679.
- 193 40. V. Anisimov and P. Paneth, ISOEFF98. A program for studies of isotope effects using  
194 Hessian modifications, *J. Math. Chem.*, 1999, **26**.
- 195 41. A. Streitwieser Jr, R. Jagow, R. Fahey and S. Suzuki, Kinetic isotope effects in the  
196 acetolyses of deuterated cyclopentyl tosylates 1, 2, *J. Am. Chem. Soc.*, 1958, **80**, 2326-  
197 2332.
- 198 42. K. Świderek and P. Paneth, Extending limits of chlorine kinetic isotope effects, *J. Org.*  
199 *Chem.*, 2012, **77**, 5120-5124.

- 200 43. L. Szatkowski and A. Dybala-Defratyka, A computational study on enzymatically driven  
201 oxidative coupling of chlorophenols: An indirect dehalogenation reaction, *Chemosphere*,  
202 2013, **91**, 258-264.
- 203 44. L. Szatkowski, R. N. Manna, A. Grzybkowska, R. Kamiński, A. Dybala-Defratyka and P.  
204 Paneth, in *Methods in enzymology*, Elsevier, 2017, vol. 596, pp. 179-215.
- 205 45. A. Siwek, R. Omi, K. Hirotsu, K. Jitsumori, N. Esaki, T. Kurihara and P. Paneth, Binding  
206 modes of DL-2-haloacid dehalogenase revealed by crystallography, modeling and isotope  
207 effects studies, *Arch. Biochem. Biophys.*, 2013, **540**, 26-32.

208